Theory of the Knight Shift and the Relaxation Time in Lead*

L. TTERLIKKIS
Institute of Molecular Biophysics, Florida State University, Tallahassee, Florida 32306

AND

S. D. MAHANTI
Bell Telephone Laboratories, Murray Hill, New Jersey 07974

AND

T. P. DAS†
Department of Physics, University of California, Riverside, California 92507

(Received 12 June 1969)

A relativistic formulation for the hyperfine interaction in metals developed in an earlier paper for alkali metals using Dirac orthoganalized-plane-wave wave functions is applied to metallic lead. The calculated values of the Knight shift K_s, (T_1T), and the Korringa constant $K_s^2T_1T/S[S=(\gamma_e/\gamma_N)^2\hbar/4\pi k_B]$, including exchange-enhancement effects are found to be 1.47%, 293×10^{-4} deg sec and 1.08, respectively. The experimental values are 1.47%, 253×10^{-4} deg sec and 0.928, respectively. Possible sources of correction to the calculated Knight shift and relaxation times are listed and analyzed.

I. INTRODUCTION

In recent years there has been considerable improvement in the understanding of the electronic structure of metals. In particular, the band structure of the nontransitional metals calculated either with an actual potential obtained from first principles or through the use of empirical potentials (pseudopotential[1] and model potential[2]) agrees reasonably well with the data from Fermi-surface measurements. It is therefore desirable to attempt a more detailed quantitative understanding of the properties depending primarily on the wave functions. The various sources of contribution to properties like the Knight shift K_s and the nuclear spin-lattice relaxation time T_1 were only qualitatively understood in the past and only recently has their quantitative evaluation become possible. Quantitative analyses of the hyperfine properties have already been made in a number of alkali[3] and second-group[4] metals. In this paper we will be concerned with a relativistic calculation of K_s and T_1 for a much heavier metal, lead. Being so heavy, relativistic effects are expected to be quite important for lead, particularly for its hyperfine properties. In an earlier paper[5] we have developed the relativistic theory for hyperfine interaction in metals and applied it to the heavier alkali metals, rubidium, and cesium. The techniques employed there can be easily extended to the case of lead which differs from the alkali metals in having more than one occupied band. The band structure of lead is believed to be well understood from both theoretical[6] and experimental[7] points of view. A rather extensive theoretical analysis[7] is available using pseudopotential techniques which predicts Fermi-surface dimensions in very good agreement with the results of de Haas–van Alphen measurements. The pseudopotential band structure results also agree well with those from less extensive augmented-plane-wave calculation.[6] Thus a quantitative analysis of K_s and T_1 is now possible and can provide a further test of the model used for the band calculation. Recently the Rudermann-Kittel and pseudodipolar interaction constants (A_{ij} and B_{ij}) have been calculated[8] in this metal and were found to be in reasonable agreement with experiment. While these latter properties are also associated with the hyperfine interaction, they involve the Rudermann-Kittel-Kasuya-Yosida (RKKY) polarization of the electrons which arises from the entire Fermi volume instead of the Fermi surface alone. The Knight shift and relaxation time, which depend on hyperfine properties associated with the Fermi surface, thus complement the information from A_{ij} and B_{ij} and it is of interest to see if one can get comparable agreement between theory and experiment for K_s and T_1.

In Sec. II, we give a brief outline of the general formalism for the relativistic treatment of K_s and T_1 with particular emphasis on the multiband nature of the system. In Sec. III, we present the results of our calculation and discuss the nature of agreement of K_s, T_1T, and the Korringa constant with experiment. The importance of other mechanisms that can contribute

* Work at Riverside supported in part by National Science Foundation.

† Present address: Department of Physics, University of Utah, Salt Lake City, Utah 84112.

[1] W. A. Harrison, *Pseudo-Potential in the Theory of Metals* (W. A. Benjamin, Inc., New York, 1964).

[2] R. W. Shaw, Jr., Ph.D. thesis, Stanford University, 1968 (unpublished), and references therein.

[3] S. D. Mahanti and T. P. Das, Phys. Rev. **183**, 674 (1969); S. D. Mahanti, Ph.D. thesis, University of California (Riverside) 1968 (unpublished).

[4] P. Jena, S. D. Mahanti, and T. P. Das, Phys. Rev. Letters **20**, 544 (1968); Phys. Rev. (to be published).

[5] L. Tterlikkis, S. D. Mahanti, and T. P. Das, Phys. Rev. **178**, 630 (1969).

[6] T. L. Loucks, Phys. Rev. Letters **14**, 1072 (1965).

[7] J. R. Anderson and A. V. Gold, Phys. Rev. **139**, A1459 (1965).

[8] L. Tterlikkis, S. D. Mahanti, and T. P. Das, Phys. Rev. Letters **21**, 1796 (1968).

to K_s and T_1T will also be briefly analyzed in terms of their bearing on the agreement between experiment and theory.

II. THEORY

The relativistic hyperfine Hamiltonian[9] is given by

$$\mathcal{H}_{\rm hyp}{}^{R}=\sum_i e\boldsymbol{\alpha}_i\cdot\mathbf{A}(\mathbf{r}_i)\,, \tag{1}$$

where

$$\mathbf{A}(\mathbf{r}_i)=\boldsymbol{\mu}_N\times\mathbf{r}_i/r_i{}^3 \tag{2}$$

is the vector potential at the site of the ith electron produced by the nuclear magnetic moment $\boldsymbol{\mu}_N$, treated as a classical dipole and located at the origin. The components of $\boldsymbol{\alpha}_i$ are the (4×4) Dirac matrices and $\mathbf{r}_i$ is the position vector of the ith electron. As is well known, the Hamiltonian in Eq. (1) reduces in the nonrelativistic limit to a sum of contact, dipolar, and orbital hyperfine interaction terms. For studying the Knight shift and relaxation times, we need the expectation values of $\mathcal{H}_{\rm hyp}{}^{R}$ over the relativistic conduction electron (Bloch-Dirac) wave functions. In our calculations, we have utilized a linear combination of Dirac-OPW (DOPW) functions, namely,

$$\Psi_{n\rho}(\mathbf{k},\mathbf{r})=\sum_{\mathbf{K}} C_{n\rho}(\mathbf{k}+\mathbf{K})\Psi_{\rm DOPW}(\mathbf{k}+\mathbf{K};\mathbf{r};\rho)\,, \tag{3}$$

where n and ρ are the band and majority spin indices. The sum in $\mathbf{K}$ is taken over an appropriate number of reciprocal-lattice vectors to obtain convergence in band energies and $\Psi_{\rm DOPW}(\mathbf{k};\mathbf{r};\rho)$ are four-component Dirac OPW functions normalized over the Wigner-Seitz volume. The DOPW's are obtained by taking four-component plane-wave functions and making them orthogonal to the core functions.

The matrix element of the hyperfine operator between two Bloch-Dirac functions is given by

$$\langle n\mathbf{k}\rho|\,e\boldsymbol{\alpha}\cdot\mathbf{A}\,|n'\mathbf{k}'\rho'\rangle=\sum_{\mathbf{K},\mathbf{K}'} C_{n\rho}{}^{*}(\mathbf{k}+\mathbf{K})C_{n'\rho'}(\mathbf{k}'+\mathbf{K}')$$
$$\times\langle\mathbf{k}+\mathbf{K},\rho|\,e\boldsymbol{\alpha}\cdot\mathbf{A}\,|\mathbf{k}'+\mathbf{K}',\rho'\rangle\,. \tag{4}$$

For both convenience of calculation and physical interpretation, it is helpful to express the DOPW's in angular spinor notation[9] and separate the contributions from various angular components of the Bloch-Dirac function to the hyperfine matrix element. Thus, the $\Psi_{\rm DOPW}(\mathbf{k};\mathbf{r};\rho)$ function can be written as

$$\Psi_{\rm DOPW}(\mathbf{k};\mathbf{r};\rho)=\sum_{\kappa\mu} a_{\kappa\mu}(\hat{k},\rho)\begin{pmatrix} b_\kappa(k,r)\Psi_{\kappa\mu}\\ id_\kappa(k,r)\Psi_{-\kappa\mu}\end{pmatrix}, \tag{5}$$

where κ is the index associated with the quantum numbers lj and

$$a_{\kappa\mu}(\hat{k},\rho)=4\pi i^{l}\left(\frac{1+E}{2E}\right)C(l\tfrac{1}{2}j;\mu-\rho,\rho)Y_l{}^{\mu-\rho*}(\hat{k})\,, \tag{6}$$

$$b_\kappa(k,r)=\left[j_l(kr)-\sum_n D_{n\kappa}(k)g_{n\kappa}(r)\right]\frac{A(\mathbf{k})}{\Omega_0{}^{1/2}}\,,$$

$$d_\kappa(k,r)=\left[\frac{kS_\kappa}{1+E}j_{l'}(kr)-\sum_n D_{n\kappa}(k)f_{n\kappa}(r)\right]\frac{A(\mathbf{k})}{\Omega_0{}^{1/2}}\,,$$

$$D_{n\kappa}(k)=\int_0^\infty\left[g_{n\kappa}(r)j_l(kr)+f_{n\kappa}(r)\frac{kS_\kappa}{1+E}j_{l'}(kr)\right]r^2dr\,. \tag{7}$$

In Eq. (7),

$$S_\kappa=1 \quad \text{for} \quad \kappa=j+\tfrac{1}{2}=l=l'+1\,,$$
$$S_\kappa=-1 \quad \text{for} \quad \kappa=-(j+\tfrac{1}{2})=-l'=-(l+1)\,.$$

E is the total energy (including the rest energy) in units of mc^2 and is nearly unity, $f_{n\kappa}(r)$ and $g_{n\kappa}(r)$ are the radial parts of the four-component core wave functions, and $A(\mathbf{k})$ is the normalization factor for the OPW wave function. The general hyperfine matrix element[5] in angular spinor representation becomes

$$\langle\mathbf{k}\rho|\,e\boldsymbol{\alpha}\cdot\mathbf{A}\,|\mathbf{k}\rho'\rangle=e\mu_z P\,, \tag{8}$$

where the various angular components of P are given in the Appendix. In obtaining Eq. (8), the nuclear moment has been assumed to point in the z direction.

In order to evaluate the hyperfine matrix elements in Eq. (4) one needs the coefficients $C_{n\rho}(\mathbf{k}+\mathbf{K})$ in the linear combination of DOPW functions. These coefficients were obtained in our calculation by a pseudopotential technique, the basis functions for the pseudofunction $\Phi_{n\rho}(\mathbf{k})$ being Dirac plane waves $\Psi_{\rm DPW}(\mathbf{k}+\mathbf{K};\mathbf{r};\rho)$.

$$\Phi_{n\rho}(\mathbf{k},\mathbf{r})=\sum_{\mathbf{K}} C_{n\rho}(\mathbf{k}+\mathbf{K})\Psi_{\rm DPW}(\mathbf{k}+\mathbf{K};\mathbf{r};\rho)\,. \tag{9}$$

The actual crystal wave functions $\Psi_{n\rho}(\mathbf{k};\mathbf{r})$ are obtained from the pseudofunctions $\Phi_{n\rho}(\mathbf{k};\mathbf{r})$ by orthogonalizing the latter to the core wave functions. This is exactly equivalent to replacing $\Psi_{\rm DPW}(\mathbf{k}+\mathbf{K};\mathbf{r};\rho)$ in Eq. (3) by $\Psi_{\rm DOPW}(\mathbf{k}+\mathbf{K};\mathbf{r};\rho)$ with $C_{n\rho}(\mathbf{k}+\mathbf{K})$ unchanged. In the pseudopotential formalism the actual crystal potential is replaced by a suitable pseudopotential

$$V^p(\mathbf{r})=\sum_{\mathbf{K}} V^p(\mathbf{K})e^{i\mathbf{K}\cdot\mathbf{r}}.$$

The coefficients $C_{n\rho}(\mathbf{k}+\mathbf{K})$ satisfy the following coupled equations in terms of the pseudopotential matrix elements:

$$T(\mathbf{k}+\mathbf{K})C(\mathbf{k}+\mathbf{K})+\sum_{\mathbf{K}'} C(\mathbf{k}+\mathbf{K}')V(\mathbf{K}-\mathbf{K}')$$
$$=E(\mathbf{k})C(\mathbf{k}+\mathbf{K})\,, \tag{10}$$

[9] M. E. Rose, *Relativistic Electron Theory* (John Wiley & Sons, Inc., New York, 1961).

where

$$T(\mathbf{k}+\mathbf{K})=\frac{\hbar^2}{2m}|\mathbf{k}+\mathbf{K}|^2, \tag{11}$$

and we have omitted the indices n,ρ for the sake of brevity. In our calculation we have utilized Anderson and Gold's[7] pseudopotential parameters which they obtain by fitting the Fermi-surface dimensions obtained from de Haas–van Alphen data using four reciprocal-lattice vectors

$$\mathbf{K}_1=(0,0,0),\quad \mathbf{K}_3=(1,1,1),$$
$$\mathbf{K}_2=(0,0,2),\quad \mathbf{K}_4=(1,\bar{1},1)$$

in Eq. (10). The use of these four $\mathbf{K}$ vectors entails the choice of two local pseudopotential parameters which were found to be

$$\begin{aligned} V(111)&=0.069,\\ V(200)&=-0.039. \end{aligned} \tag{12}$$

In addition to this choice, Anderson and Gold[7] have obtained another set of pseudopotential coefficients where the spin-orbit effect was included through an additional parameter. For the points on the Fermi surface from which most contribution to K_s and T_1 is expected, spin-orbit effects were not found to be significant. Furthermore, the main relativistic effects on the matrix elements of hyperfine interaction occur in the region near the nucleus and these are substantially included in our calculation by the replacement of non-relativistic OPW's by four-component Dirac OPW functions. The choice of the pseudopotential parameters in Eq. (12) that we have utilized was, therefore, felt to be quite adequate for our purpose.

In contrast to recent work[2] on cadmium and zinc, Anderson and Gold[7] did not use nonlocal terms in their pseudopotential. The largest nonlocality effect in these metals comes from the influence of the outermost cores which are diffused. In lead, the outermost core electrons occupy the $5d$ orbitals. Since there are four band electrons outside of the $5d$ orbitals in lead, these are expected to be significantly less shielded and therefore more tightly bound relative to the d electrons in the divalent metals. Thus, the neglect of nonlocal pseudopotential terms in lead is not expected to have as serious an effect as it would have in zinc and cadmium.

For a multiband system where the different pieces of the Fermi surface are associated with different bands, the expression for the Knight shift is given by

$$K_s=\chi_s\sum_n \omega_n\Phi_n(\epsilon_F), \tag{13}$$

where χ_s is the total spin susceptibility from all the bands without including exchange-enhancement effects. Using the calculated density of states[7] one obtains

$$\chi_s=1.01\times10^{-6}\text{ cgs vol units}. \tag{14}$$

In Eq. (13) the sum over n refers only to the occupied bands. In lead, only the second and third bands contribute, since the first band is completely full and does not contribute to the Fermi surface. The weighting factors in Eq. (13), ω_n, are the ratios of the density of states from the nth-band Fermi surface to the total density of states at the Fermi surface. The quantity $\Phi_n(\epsilon_F)$ is the averaged spin density from the nth-band Fermi surface:

$$\Phi_n(\epsilon_F)=\sum_i t_i g_n{}^i(\epsilon_F)\Phi_n{}^i(\epsilon_F)/\sum_i t_i g_n{}^i(\epsilon_F). \tag{15}$$

In Eq. (15) the summation over i refers to the sample points on each band chosen in the averaging procedure, t_i is the geometric factor associated with the symmetry of the sample point i, and $g_n{}^i(\epsilon_F)=|\nabla_{\mathbf{k}i}\epsilon_F|_n{}^{-1}$ is the local density of states for this point. The quantities $\Phi_n{}^i(\epsilon_F)$ in Eq. (15) for different points i on the nth band are calculated using Eq. (8) and results given in the Appendix for the hyperfine matrix elements and the relation

$$\Phi_n{}^i(\epsilon_F)=\Phi_n(k_F{}^i,k_F{}^i)=-(2mc/\hbar)P. \tag{16}$$

The number of points i and their locations are chosen to enable a judicious sampling of each band in calculating the average in Eq. (15).

The analysis of $(T_1T)^{-1}$ for a many-band system is somewhat subtle. By a simple extension of the procedure for deriving relaxation times for single-band systems, one obtains for the direct-contact contribution

$$(T_1T)^{-1}=\frac{2\pi}{\hbar}k_B\sum_{nk_F\rho}\sum_{n'k_F'\rho'}g_n(\epsilon_{kF})g_{n'}(\epsilon_{kF'})\times|\langle n\mathbf{k}_F\rho|\mathcal{H}_{\rm hyp}{}^R|n'\mathbf{k}_F'\rho'\rangle|^2, \tag{17}$$

where the sums over $n\mathbf{k}_F\rho$ and $n'\mathbf{k}_F'\rho'$ refer to points on the Fermi surface. If the hyperfine matrix element $\langle n\mathbf{k}_F\rho|\mathcal{H}_{\rm hyp}{}^R|n'\mathbf{k}_F'\rho'\rangle$ could be separated into two parts as in

$$\langle n\mathbf{k}_F\rho|\mathcal{H}_{\rm hyp}{}^R|n'\mathbf{k}_F'\rho'\rangle=f(n\mathbf{k}_F\rho)f(n'\mathbf{k}_F'\rho'), \tag{18}$$

then Eq. (17) for $(T_1T)^{-1}$ would reduce to

$$(T_1T)^{-1}=\frac{2\pi}{\hbar}k_B|\sum_{nk_F\rho}g_n(\epsilon_{kF}\rho)f(n\mathbf{k}_F)f(n\mathbf{k}_F\rho)|^2$$
$$=\frac{2\pi}{\hbar}k_B|\sum_{n\mathbf{k}_F\rho}g_n(\epsilon_{kF})\langle n\mathbf{k}_F\rho|\mathcal{H}_{\rm hyp}{}^R|n\mathbf{k}_F\rho\rangle|^2. \tag{19}$$

Comparing Eqs. (13) and (19) for K_s and $(T_1T)^{-1}$, we see that the Korringa relation would hold only when an approximation of the form (18) is valid. In addition, the exchange enhancement of the susceptibility[10] and

[10] C. Herring, in *Magnetism*, edited by G. T. Rado and H. Suhl (Academic Press Inc., New York, 1966), Vol. IV.

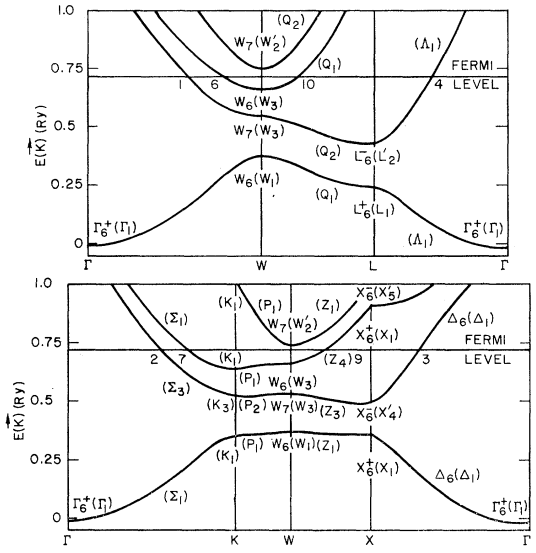

FIG. 1. Energy bands and Fermi level for lead as calculated by Anderson and Gold. The points on the Fermi surface, utilized for the calculation of hyperfine matrix elements (excepting 5 and 8 along the ΓU line) are shown in the figure.

core-polarization effects[11] have to be ignored for the Korringa relation to be satisfied. The relation (18) holds exactly for the direct term in nonrelativistic theory where only the contact interaction is effective. An examination of the relativistic matrix elements (see Appendix) indicates that the presence of non-s-like contributions in addition to the s-like ones can lead to a departure from the relation (18) and hence from the Korringa relation. An assessment of the extent of this departure can be made from an examination of the relative importance of the non-s-like contributions to the hyperfine matrix elements as compared to the s-like one. This type of departure from the Korringa relation is very similar to that one gets from core-polarization effects.[11]

III. RESULTS AND DISCUSSION

The band structure of lead calculated using the Anderson and Gold[7] pseudopotential parameter is reproduced in Fig. 1. The first band is seen, from these figures, to be completely full and therefore does not contribute to the Fermi surface. The Fermi surface derives contributions primarily from the second and third bands and a small pocket of electrons near the W point in the fourth band. The points that we chose in obtaining our Fermi surface average are numbered from 1 to 10 and their coordinates, symmetry and other relevant features are listed in Table I. The corresponding hyperfine matrix elements are given in Table II. For the purpose of later discussion we have separated the contributions from the conduction electrons into ($s_{1/2}$-$s_{1/2}$) and ($p_{1/2}$-$p_{1/2}$, $p_{3/2}$-$p_{3/2}$, and $p_{1/2}$-$p_{3/2}$) parts. In the nonrelativistic theory, the $s_{1/2}$-$s_{1/2}$ part goes over to the usual Fermi contact term and the rest of the terms vanish. The physical origin of the total of the latter terms, and indeed that from all the non-s components of the wave functions can, therefore, best be understood by looking at these non-s terms from a perturbation point of view. Thus, in Pauli-relativistic theory these terms may be considered to arise from the combined effect of

$$\sum_i \frac{\mathbf{\mu}_N \cdot \mathbf{l}_i}{r_i^3}, \quad \sum_i \xi(r_i)\mathbf{l}_i \cdot \mathbf{s}_i, \quad \text{and} \quad \sum_i \mathbf{s}_i \cdot \mathbf{H}.$$

This mechanism leads to an effective hyperfine field at the nucleus which is proportional to both the applied field (through Pauli paramagnetism) and the strength of the spin-orbit interaction.

From Table II, it is seen that whenever the $s_{1/2}$-$s_{1/2}$ contribution is nonzero, the first term completely dominates the rest. When the wave function is purely p-like leading to $W_{\uparrow\uparrow}=0$, the entire contribution comes through the effective third-order mechanism mentioned in the last paragraph.

In the last column of Table I, we have tabulated the local density-of-states factor $|\nabla_{ki}\epsilon_F|^{-1}$ and it appears that the departure from the free-electron value is not significant excepting at a few points along the ΓX, ΓL, and ΓU directions. In carrying out the averaging in Eq. (15) over the Fermi surface one has either to carry out a detailed scanning of the Fermi surface which is rather laborious, or choose representative points on various pieces of the Fermi surface and average according to relative surface areas of these various pieces. The finer the division into pieces, the more accurate is the averaging procedure. However, in the absence of a detailed knowledge (both theoretical and experimental) of the Fermi surface that is required for a fine scanning, we have carried out the averaging procedure for each band (1 and 2) separately. Only the points lying along the ΓX and ΓL lines and along the $WX(Z)$ and $WL(Q)$ lines have been included in the averaging procedure. This sampling may be seen to be rather good by examining the Fermi surface obtained by Anderson and Gold,[7] major portions of which lie along these symmetry directions. Finally, while carrying out the

TABLE I. Specification of points chosen on the Fermi surface for the calculation of average spin density.

No.	Coordinate	Symmetry line	Symmetry factor	Band	$g_i(\epsilon_F)$[a]
1	(0.193,0,0.386)	ΓW	24	2	0.9960
2	(0.298,0,0.298)	ΓK	12	2	1.0072
3	(0,0,0.482)	ΓX	6	2	0.6897
4	(0.19,0.19,0.19)	ΓL	8	2	0.6166
5	(0.10,0.10,0.40)	ΓU	24	2	0.7058
6	(0.247,0,0.494)	ΓW	24	3	1.0652
7	(0.35, 0,0.35)	ΓK	12	3	1.0764
8	(0.14,0.14,0.14)	ΓU	24	3	0.9029
9	(0.209,0,0.679)	WX	6	3	1.0570
10	(0.339,0.117,0.562)	WL	8	3	0.9185

[a] $g_i(\epsilon_F)$ is the local density of states.

[11] Y. Yafet and V. Jaccarino, Phys. Rev. **133**, A1630 (1964).

TABLE II. Relativistic hyperfine matrix elements (expressed in units of χ_s) in the K_s expression. The entries in columns 3–8 include the numerical factors of Eqs. (A3)–(A6) and $-2mc/\hbar$ of Eq. (16).

No.	Normalization constant	I $W_{\bar{1}\bar{1}}$	II $W_{\bar{2}\bar{2}}$	III W_{11}	IV $W_{\bar{2}1}+W_{1\bar{2}}$	Sum II+III+IV	$\Phi^i(\epsilon_F)$[a] I+II+III+IV
1	1.0129	28093	724	654	−510	868	28961
2	1.0088	24825	638	689	−464	863	25688
3	1.0105	24020	660	1720	−631	1749	25769
4	0.9983	14275	742	−106	−407	229	14504
5	1.0065	21629	802	74	−407	499	22098
6	0.9841	0	1023	−2000	−292	−1269	−1269
7	0.9841	0	1029	−2010	−294	−1276	−1276
8	0.9851	1969	681	−293	−345	43	2012
9	0.9951	0	1120	−2189	−320	−1389	−1389
10	0.9851	10785	825	51	−473	403	11188

[a] $\Phi^i(\epsilon_F)$ does not include the normalization factor.

averaging for individual bands, the proper geometrical structure factors represented by t_i in our Table I have been included.

In the absence of any directly measured experimental value of χ_s from electron spin-resonance measurements, we have utilized the value given in Eq. (14) obtained from the calculated density of states. The theoretical density of states, after correcting for the electron-phonon interaction effects, agrees very well with that obtained from specific-heat measurements. Using a value for $\chi_s=1.01\times10^{-6}$ cgs vol units derived in this manner, we have obtained K_s listed in Table III. Out of the total 1.23%, the second and third bands contribute 0.62 and 0.61%, respectively.

The second-band contribution to K_s is seen to be nearly equal to that from the third band although the latter gives a larger density of states at the Fermi surface. The major reason for this is the large amount of p character in the third band, particularly along the Z line. It was for this reason also that the third-band contribution to the Ruderman-Kittel parameter was found[8] to be small. Our calculated value of K_s is 1.23%.

Before proceeding to the calculation of T_1T, we would like to summarize briefly the present experimental situation[12] for K_s and T_1. Snodgrass and Bennett[13] have measured the Knight shift. Their value of K_s is 1.47% compared to 1.24% obtained by Knight[14] and Rowland[15] in earlier measurements. The apparent large discrepancy between the two experimental values has been ascribed to the uncertainties in the shielding associated with the reference compound. However, a considerable amount of work has been done on the chemical shifts of lead salts with lead metal as the reference material. If one chooses the most diamagnetic salt as the reference material, then the experimental value of K_s is found to range between 1.46 and 1.48%. This appears to be a reasonable choice for the experimental value of K_s to compare with theory. As regards the experimental value of T_1, Snodgrass and Bennett[13] utilized the temperature dependence of the linewidth, the temperature independence of the spin-spin relaxation time T_2', and the Korringa relation to obtain $T_1=360$ μsec at 77°K. From their pulsed NMR experiments which provide a more direct measurement, Asayama and Itoh[16] have obtained for T_1 a value of 380 μsec at the same temperature. The latest experimental measurement of T_1 is by Dickson[17] who, also using pulsed NMR technique, finds $T_1=329$ μsec. For the comparison of our theoretical values, we shall utilize Dickson's[17] value which gives

$$(T_1T)_{\text{expt}}=253.3\times10^{-4}\ \text{deg sec}. \tag{20}$$

To calculate the relaxation time, strictly speaking, one has to use Eq. (17). This would entail rather complicated numerical computations since Eq. (17) involves interband matrix elements. However, as discussed in Sec. II, under certain conditions one can utilize the simpler Eq. (19). A particular criterion for this is that the relativistic terms that lead to s-contact interaction in the nonrelativistic limit predominate strongly over the matrix elements of non-s angular character. This is indeed seen to be true from Table II and so we have utilized the Eq. (19) for obtaining T_1T. The contributions to $(T_1T)^{-1}$ can no longer be split into separate parts associated with each of the two bands because Eq. (19) involves the square of the sum

TABLE III. Theoretical values of K_s, T_1T, and $K_s^2T_1T/S$ [$S=(\hbar/4\pi k_B)(\gamma_e/\gamma_N)^2$], with and without the inclusion of exchange-enhancement effects and available experimental results.

	Without exchange enhancement	With exchange enhancement[a]	Experiment
K_s (in units of 10^{-2})	1.23	1.47	1.47[b]
(T_1T) (10^{-4} deg sec)	389.8	293.1	253.3[c]
$K_s^2T_1T/S$	1.0	1.08	0.928

[a] Using expressions of Silverstein, Ref. 18, for χ_s and Moriya, Ref. 19, for $\chi(q,0)$.
[b] R. J. Snodgrass and L. H. Bennett, Ref. 13.
[c] E. M. Dickson, Ref. 17.

[12] We are grateful to the referee for making the experimental status of K_s and T_1T clear to us.
[13] R. J. Snodgrass and L. H. Bennett, Phys. Rev. **132**, 1465 (1963).
[14] W. D. Knight, in *Solid State Physics*, edited by F. Seitz and D. Turnbull (Academic Press Inc., New York, 1956).
[15] T. J. Rowland, Progr. Mat. Sci. **9**, 1 (1961).
[16] K. Asayama and J. Itoh, J. Phys. Soc. Japan **17**, 1065 (1962).
[17] E. M. Dickson, Ph.D. thesis, University of California, Berkeley, 1968 (unpublished).

of terms from the two bands. The total calculated value of T_1T was found to be 389×10^{-4} deg sec at 77°K, as shown in Table III. This value is larger than all three experimental values. Using Dickson's[17] value 253.3×10^{-4} deg sec at the same temperature as the standard one, we find that the theoretical value is about 1.54 times larger than experiment. The theoretical Korringa constant, by virtue of the way we obtain T_1, is exactly equal to Korringa's value

$$S=(K_s^2T_1T)_{\text{free}}=589.83\times10^{-8}. \tag{21}$$

Using the experimental values[13,17] of K_s and T_1, one obtains

$$(K_s^2T_1T)_{\text{expt}}=547.35\times10^{-8}. \tag{22}$$

The experimental values of K_s and $(T_1T)^{-1}$ are found to be significantly larger than theory while the experimental Korringa constant is about 7% lower than the free-electron value in Eq. (21). In trying to analyze the source of the difference between theory and experiment, it is best to consider all three quantities, K_s, T_1, and the Korringa constant, simultaneously. Three important additional sources of contribution to these quantities are hyperfine fields associated with core-polarization and orbital effects and the exchange enhancement of χ_s. Considering the last of these effects first, this corresponds to the combined effects of exchange and correlation between the electrons and the external field. The complexity of the problem is compounded by the presence of more than one occupied band. In the absence of a better alternative and for the purpose of making semiquantitative estimates, one can utilize Silverstein's[3,18] and Moriya's[3,19] enhancement factors for these quantities which were derived for a uniform electron gas in the effective-mass approximation. It is appropriate to stress the reservation here that the approximate expressions for the exchange enhancements of K_s and $(T_1T)^{-1}$ were derived for a system of free-electron gas using the RPA[10] approximation and are therefore not adequate to make a complete quantitative evaluation of the enhancement effects in real systems.

The calculation of the Silverstein enhancement factor requires a knowledge of the ratio m^*/m, m^* being the thermal mass related to the density of states at the Fermi surface (without electron-phonon correction) and r_s, the electron sphere radius for the metal. From Anderson and Gold's[7] density of states

$$m^*/m=0.89 \tag{23}$$

and remembering that there are four valence electrons in lead, $r_s=(4)^{-1/3}r_{ws}=2.281\ a_0$, where r_{ws} is the Wigner-Seitz radius. Using Silverstein's[18] expression, one then gets for the enhancement factor to the susceptibility

$$\frac{\chi_s}{\chi_{\text{band}}}=\frac{1}{1-\alpha_{\text{band}}}=1.196. \tag{24}$$

A test of the validity of this approximation for the enhancement factor would be possible if a direct spin-resonance measurement of χ_s were available to compare with the theoretical value. The enhancement factor in Eq. (24) was also applied to K_s, leading to

$$K_s=1.47\%. \tag{25}$$

To get the enhancement factor for $(T_1T)^{-1}$ we have made use of Moriya's[19] expression together with $\alpha_{\text{band}}=0.164$ derived from Eq. (24). This procedure leads to an enhancement factor of 1.327 for $(T_1T)^{-1}$ which leads to a corrected value for T_1T,

$$(T_1T)=293.1\times10^{-4}\text{ deg sec}, \tag{26}$$

and the Korringa constant

$$(K_s^2T_1T)_{\text{theor}}=633.4\times10^{-8}. \tag{27}$$

The effect of the inclusion of exchange-enhancement effects is thus seen from Table III to improve the values of K_s and T_1 in the direction of experiment, with the former in almost exact agreement with experiment. The theoretical value of T_1T and $K_s^2T_1T$ are both roughly 1.16 times larger than the experiment.

The remaining discrepancy between theory and experiment for T_1T could be explained as either in improvement of the theory for exchange enhancement or in inclusion of additional mechanisms that can contribute to the hyperfine field at the nucleus. Among the latter is the exchange core-polarization (ECP) mechanism[3,11,20] involving the core electrons interacting with the surplus spin electrons at the Fermi surface in the presence of the magnetic field. A proper treatment of this ECP effect requires a relativistic adaptation of the currently used moment-perturbation procedure for handling this effect.[3,20] In the absence of actual calculations, one can only speculate on the possible importance of the ECP effect. What is needed is a mechanism that will retain the good agreement of the Knight shift with experiment, but reduce the relaxation time. The ECP effect can achieve this objective only if the contributions to it from the s and p components of the conduction-electron wave functions substantially cancel, as in both lithium[20] and beryllium[4] while contributions to the relaxation rates from the various angular components have the same sign and add up.[3,11] This is an attractive possibility in view of the substantial p character in the third band of lead, but cannot be decided upon without actual calculation.

The orbital hyperfine interaction offers another avenue for improved agreement between theory and

[18] S. D. Silverstein, Phys. Rev. **128**, 631 (1962); **130**, 912 (1963).
[19] T. Moriya, J. Phys. Soc. Japan **18**, 516 (1963).
[20] W. M. Shyu, G. D. Gaspari, and T. P. Das, Phys. Rev. **141**, 603 (1966); **152**, 270 (1966).

experiment. Orbital contributions[11,21–23] to the Knight shift and relaxation rate can be quite significant in view of the pronounced p character in the third band. Further, there are important differences in the processes that contribute to the Knight shift and T_1T. Thus, the orbital Knight shift involves virtual transitions from all the occupied states below the Fermi surface while the relaxation process requires real transitions from the Fermi surface. Additionally, the Knight-shift process involves a periodic perturbation in the presence of an external uniform magnetic field and thus is composed of vertical transitions in k space[21] while the relaxation process, produced by the localized field of the nuclear magnet, is not subject to this restriction. As a consequence of these differences, it is not unlikely[23] that the relative importance of the orbital contributions to the relaxation rate could be more pronounced than for the Knight shift.

In addition to these mechanisms, various mechanisms involving spin-orbit effects could also contribute to the Knight shift and relaxation rate. One possibility for the Knight shift is the third-order process involving one order in the Fermi-contact interaction, one order in spin-orbit, and one in the electron-orbit–magnetic-field interaction and a corresponding process for the relaxation effect with the electron-orbit magnetic field replaced by electron-orbit–nuclear-moment interaction. Spin-orbit effects are important for a heavy metal like lead and are directly contained in a relativistic theory, but the effects of the other perturbations have to be worked out. A parallel mechanism involving replacement of the electron-orbit–magnetic-field perturbation by electron-spin–magnetic-field interaction is already included in the present relativistic analysis. It is thus clear that there are several additional mechanisms which require complicated calculations and need to be included if improvement over the present theoretical results is desired in terms of exact quantitative comparison with experiment. Our results indicate, however, that a relativistic treatment of direct hyperfine effects does explain major parts of K_s and $(T_1T)^{-1}$. This is very encouraging and suggests that an adaptation of the present relativistic analysis to other heavy metals and to heavy-metal alloys should be very useful for understanding resonance data in such systems.

ACKNOWLEDGMENTS

We are extremely thankful to Dr. E. M. Dickson, Dr. H. Alloul, and Professor C. Froidevaux for communicating their experimental results prior to publication, and to Dr. E. M. Dickson for many interesting and helpful discussions.

[21] R. Kubo and Y. Obata, J. Phys. Soc. Japan **11**, 547 (1956); Y. Obata, *ibid.* **18**, 1020 (1963).
[22] R. J. Noer and W. D. Knight, Rev. Mod. Phys. **36**, 177 (1966); A. M. Clogston, A. C. Gossard, V. Jaccarino, and Y. Yafet, *ibid.* **36**, 170 (1964).
[23] J. A. Setchick, A. V. Gossard, and V. Jaccarino, Phys. Rev. **136**, A1119 (1964).

APPENDIX: GENERAL MATRIX ELEMENT OF THE HYPERFINE OPERATOR

The general matrix element can be divided into two basic categories; one diagonal in the spin space ($\rho=\rho'$) and the other off diagonal in the spin space ($\rho=-\rho'$).

Case 1:

$$\rho=\rho'=\tfrac{1}{2}, \tag{A1}$$

$$P=P_{\bar{1}\bar{1}}+P_{\bar{2}\bar{2}}+P_{11}+P_{1\bar{2}}+P_{\bar{2}1}+\cdots, \tag{A2}$$

where the $(\bar{1}\bar{1})$, $(\bar{2}\bar{2})$, (11), $(1\bar{2})$, and $(\bar{2}1)$, etc., terms represent, respectively, the contributions $s_{1/2}-s_{1/2}$, $p_{3/2}-p_{3/2}$, $p_{1/2}-p_{1/2}$, $p_{1/2}-p_{3/2}$, and $p_{3/2}-p_{1/2}$, etc., between various (lj) components of the OPW functions and are given by

$$P_{\bar{1}\bar{1}}=N(\mathbf{k})N(\mathbf{k}')(8\pi/3)[W_{\bar{1}\bar{1}}(k,k')+W_{\bar{1}\bar{1}}(k',k)], \tag{A3}$$

$$\begin{aligned}P_{\bar{2}\bar{2}}=&N(\mathbf{k})N(\mathbf{k}')(4/45)(4\pi)^2\\&\times[W_{\bar{2}\bar{2}}(k,k')+W_{\bar{2}\bar{2}}(k',k)]\\&\times[2Y_1^0(\hat{k})Y_1^{0*}(\hat{k}')-Y_1^{-1}(\hat{k})Y_1^{-1*}\\&\qquad\times(\hat{k}')-9Y_1^1(\hat{k})Y_1^{1*}(\hat{k}')],\end{aligned} \tag{A4}$$

$$\begin{aligned}P_{11}=&N(\mathbf{k})N(\mathbf{k}')\tfrac{1}{9}(4\pi)^2[W_{11}(k,k')+W_{11}(k',k)]\\&\times[4Y_1^{-1}(\hat{k})Y_1^{-1*}(\hat{k}')-2Y_1^0(\hat{k})Y_1^{0*}(\hat{k}')],\end{aligned} \tag{A5}$$

$$\begin{aligned}P_{1\bar{2}}+P_{\bar{2}1}=&N(\mathbf{k})N(\mathbf{k}')(2/9)(4\pi)^2[W_{1\bar{2}}(k,k')\\&+W_{\bar{2}1}(k,k')+W_{1\bar{2}}(k,k')+W_{1\bar{2}}(k',k)]\\&\times[Y_1^0(\hat{k})Y_1^{0*}(\hat{k}')+Y_1^{-1}(\hat{k})Y_1^{-1*}(\hat{k}')],\end{aligned} \tag{A6}$$

where $N(\mathbf{k})$ in above equations is the normalizing constant for the OPW's and

$$W_{\kappa_1\kappa_2}(k,k')=\int_0^\infty b_{\kappa_1}^*(k,r)d_{\kappa_2}(k',r)dr. \tag{A7}$$

Case 2:

$$\rho=-\rho'=\tfrac{1}{2}. \tag{A8}$$

In this case, there is no contribution from the s part of the wave function and

$$P=P_{\bar{2}\bar{2}}+P_{11}+P_{\bar{2}1}+P_{1\bar{2}}+\cdots, \tag{A9}$$

where $\bar{2}\bar{2}$, etc., have the same meaning as before and

$$\begin{aligned}P_{\bar{2}\bar{2}}=&N(\mathbf{k})N(\mathbf{k}')(4\sqrt{2}/45)(4\pi)^2\\&\times[W_{\bar{2}\bar{2}}(k,k')+W_{\bar{2}\bar{2}}(k',k)]\\&\times[Y_1^0(\hat{k})Y_1^{1*}(\hat{k}')-Y_1^{-1}(\hat{k})Y_1^{0*}(\hat{k}')],\end{aligned} \tag{A10}$$

$$\begin{aligned}P_{11}=&N(\mathbf{k})N(\mathbf{k}')(2\sqrt{2}/9)(4\pi)^2\\&\times[W_{11}(k,k')+W_{11}(k',k)]\\&\times[Y_1^0(\hat{k})Y_1^{1*}(\hat{k}')-Y_1^{-1}(\hat{k})Y_1^{0*}(\hat{k}')],\end{aligned} \tag{A11}$$

$$\begin{aligned}P_{\bar{2}1}+P_{1\bar{2}}=&N(\mathbf{k})N(\mathbf{k}')\tfrac{1}{9}\sqrt{2}(4\pi)^2\\&\times[-(W_{\bar{2}1}(k,k')+W_{\bar{2}1}(k',k))(2Y_1^0(\hat{k})Y_1^{1*}(\hat{k}')\\&+Y_1^{-1}(\hat{k})Y_1^{0*}(\hat{k}'))+(W_{1\bar{2}}(k,k')+W_{1\bar{2}}(k',k))\\&\times(Y_1^0(\hat{k})Y_1^{1*}(\hat{k}')+2Y_1^{-1}(\hat{k})Y_1^{0*}(\hat{k}'))].\end{aligned} \tag{A12}$$